Measurement of the $t\bar{t}$ Production Cross Section in $p\bar{p}$ Collisions at $\sqrt{s} = 1.96$ TeV Using Dilepton Events

D. Acosta,[15] T. Affolder,[8] T. Akimoto,[53] M. G. Albrow,[14] D. Ambrose,[42] S. Amerio,[41] D. Amidei,[32] A. Anastassov,[49] K. Anikeev,[30] A. Annovi,[43] J. Antos,[1] M. Aoki,[53] G. Apollinari,[14] T. Arisawa,[55] J-F. Arguin,[31] A. Artikov,[12] W. Ashmanskas,[2] A. Attal,[6] F. Azfar,[40] P. Azzi-Bacchetta,[41] N. Bacchetta,[41] H. Bachacou,[27] W. Badgett,[14] A. Barbaro-Galtieri,[27] G. J. Barker,[24] V. E. Barnes,[45] B. A. Barnett,[23] S. Baroiant,[5] M. Barone,[16] G. Bauer,[30] F. Bedeschi,[43] S. Behari,[23] S. Belforte,[52] G. Bellettini,[43] J. Bellinger,[57] D. Benjamin,[13] A. Beretvas,[14] A. Bhatti,[47] M. Binkley,[14] D. Bisello,[41] M. Bishai,[14] R. E. Blair,[2] C. Blocker,[4] K. Bloom,[32] B. Blumenfeld,[23] A. Bocci,[47] A. Bodek,[46] G. Bolla,[45] A. Bolshov,[30] P. S. L. Booth,[28] D. Bortoletto,[45] J. Boudreau,[44] S. Bourov,[14] C. Bromberg,[33] E. Brubaker,[27] J. Budagov,[12] H. S. Budd,[46] K. Burkett,[14] G. Busetto,[41] P. Bussey,[18] K. L. Byrum,[2] S. Cabrera,[13] P. Calafiura,[27] M. Campanelli,[17] M. Campbell,[32] A. Canepa,[45] M. Casarsa,[52] D. Carlsmith,[57] S. Carron,[13] R. Carosi,[43] A. Castro,[3] P. Catastini,[43] D. Cauz,[52] A. Cerri,[27] C. Cerri,[43] L. Cerrito,[22] J. Chapman,[32] C. Chen,[42] Y. C. Chen,[1] M. Chertok,[5] G. Chiarelli,[43] G. Chlachidze,[12] F. Chlebana,[14] I. Cho,[26] K. Cho,[26] D. Chokheli,[12] M. L. Chu,[1] S. Chuang,[57] J. Y. Chung,[37] W-H. Chung,[57] Y. S. Chung,[46] C. I. Ciobano,[22] M. A. Ciocci,[43] A. G. Clark,[17] D. Clark,[4] M. Coca,[46] A. Connolly,[27] M. Convery,[47] J. Conway,[49] M. Cordelli,[16] G. Cortiana,[41] J. Cranshaw,[51] J. Cuevas,[9] R. Culbertson,[14] C. Currat,[27] D. Cyr,[57] D. Dagenhart,[4] S. Da Ronco,[41] S. D'Auria,[18] P. de Barbaro,[46] S. De Cecco,[48] G. De Lentdecker,[46] S. Dell'Agnello,[16] M. Dell'Orso,[43] S. Demers,[46] L. Demortier,[47] M. Deninno,[3] D. De Pedis,[48] P. F. Derwent,[14] C. Dionisi,[48] J. R. Dittmann,[14] P. Doksus,[22] A. Dominguez,[27] S. Donati,[43] M. Donega,[17] M. D'Onofrio,[17] T. Dorigo,[41] V. Drollinger,[35] K. Ebina,[55] N. Eddy,[22] R. Ely,[27] R. Erbacher,[14] M. Erdmann,[24] D. Errede,[22] S. Errede,[22] R. Eusebi,[46] H-C. Fang,[27] S. Farrington,[28] I. Fedorko,[43] R. G. Feild,[58] M. Feindt,[24] J. P. Fernandez,[45] C. Ferretti,[32] R. D. Field,[15] I. Fiori,[43] G. Flanagan,[33] B. Flaugher,[14] L. R. Flores-Castillo,[44] A. Foland,[19] S. Forrester,[5] G. W. Foster,[14] M. Franklin,[19] H. Frisch,[11] Y. Fujii,[25] I. Furic,[30] A. Gajjar,[28] A. Gallas,[36] J. Galyardt,[10] M. Gallinaro,[47] M. Garcia-Sciveres,[27] A. F. Garfinkel,[45] C. Gay,[58] H. Gerberich,[13] D. W. Gerdes,[32] E. Gerchtein,[10] S. Giagu,[48] P. Giannetti,[43] A. Gibson,[27] K. Gibson,[10] C. Ginsburg,[57] K. Giolo,[45] M. Giordani,[52] G. Giurgui,[10] V. Glagolev,[12] D. Glenzinski,[14] M. Gold,[35] N. Goldschmidt,[32] D. Goldstein,[6] J. Goldstein,[40] G. Gomez,[9] G. Gomez-Ceballos,[30] M. Goncharov,[50] O. González,[45] I. Gorelov,[35] A. T. Goshaw,[13] Y. Gotra,[44] K. Goulianos,[47] A. Gresele,[3] C. Grosso-Pilcher,[11] M. Guenther,[45] J. Guimaraes de Costa,[19] C. Haber,[27] K. Hahn,[42] S. R. Hahn,[14] E. Halkiadakis,[46] R. Handler,[57] F. Happacher,[16] K. Hara,[53] M. Hare,[54] R. F. Harr,[56] R. M. Harris,[14] F. Hartmann,[24] K. Hatakeyama,[47] J. Hauser,[6] C. Hays,[13] H. Hayward,[28] E. Heider,[54] B. Heinemann,[28] J. Heinrich,[42] M. Hennecke,[24] M. Herndon,[23] C. Hill,[8] D. Hirschbuehl,[24] A. Hocker,[46] K. D. Hoffman,[11] A. Holloway,[19] S. Hou,[1] M. A. Houlden,[28] B. T. Huffman,[40] Y. Huang,[13] R. E. Hughes,[27] J. Huston,[33] K. Ikado,[55] J. Incandela,[8] G. Introzzi,[43] M. Iori,[48] Y. Ishizawa,[53] C. Issever,[8] A. Ivanov,[46] Y. Iwata,[21] B. Iyutin,[30] E. James,[14] D. Jang,[49] J. Jarrell,[35] D. Jeans,[48] H. Jensen,[14] E. J. Jeon,[26] M. Jones,[45] K. K. Joo,[26] S. Jun,[10] T. Junk,[22] T. Kamon,[50] J. Kang,[32] M. Karagoz Unel,[36] P. E. Karchin,[56] S. Kartal,[14] Y. Kato,[39] Y. Kemp,[24] R. Kephart,[14] U. Kerzel,[24] V. Khotilovich,[50] B. Kilminster,[37] D. H. Kim,[26] H. S. Kim,[22] J. E. Kim,[26] M. J. Kim,[10] M. S. Kim,[26] S. B. Kim,[26] S. H. Kim,[53] T. H. Kim,[30] Y. K. Kim,[11] B. T. King,[28] M. Kirby,[13] L. Kirsch,[4] S. Klimenko,[15] B. Knuteson,[30] B. R. Ko,[13] H. Kobayashi,[53] P. Koehn,[37] D. J. Kong,[26] K. Kondo,[55] J. Konigsberg,[15] K. Kordas,[31] A. Korn,[30] A. Korytov,[15] K. Kotelnikov,[34] A. V. Kotwal,[13] A. Kovalev,[42] J. Kraus,[22] I. Kravchenko,[30] A. Kreymer,[14] J. Kroll,[42] M. Kruse,[13] V. Krutelyov,[50] S. E. Kuhlmann,[2] N. Kuznetsova,[14] A. T. Laasanen,[45] S. Lai,[31] S. Lami,[47] S. Lammel,[14] J. Lancaster,[13] M. Lancaster,[29] R. Lander,[5] K. Lannon,[37] A. Lath,[49] G. Latino,[35] R. Lauhakangas,[20] I. Lazzizzera,[41] Y. Le,[23] C. Lecci,[24] T. LeCompte,[2] J. Lee,[26] J. Lee,[46] S. W. Lee,[50] N. Leonardo,[30] S. Leone,[43] J. D. Lewis,[14] K. Li,[58] C. Lin,[58] C. S. Lin,[14] M. Lindgren,[6] T. M. Liss,[22] D. O. Litvintsev,[14] T. Liu,[14] Y. Liu,[17] N. S. Lockyer,[42] A. Loginov,[34] M. Loreti,[41] P. Loverre,[48] R-S. Lu,[1] D. Lucchesi,[41] P. Lukens,[14] L. Lyons,[40] J. Lys,[27] R. Lysak,[1] D. MacQueen,[31] R. Madrak,[19] K. Maeshima,[14] P. Maksimovic,[23] L. Malferrari,[3] G. Manca,[28] R. Marginean,[37] M. Martin,[23] A. Martin,[58] V. Martin,[36] M. Martínez,[14] T. Maruyama,[11] H. Matsunaga,[53] M. Mattson,[56] P. Mazzanti,[3] K. S. McFarland,[46] D. McGivern,[29] P. M. McIntyre,[50] P. McNamara,[49] R. McNulty,[28] S. Menzemer,[30] A. Menzione,[43] P. Merkel,[14] C. Mesropian,[47] A. Messina,[48] T. Miao,[14] N. Miladinovic,[4] L. Miller,[19] R. Miller,[33] J. S. Miller,[32] C. Mills,[8] R. Miquel,[27] S. Miscetti,[16] G. Mitselmakher,[15] A. Miyamoto,[25] Y. Miyazaki,[39] N. Moggi,[3] B. Mohr,[6] R. Moore,[14] M. Morello,[43] T. Moulik,[45] A. Mukherjee,[14] M. Mulhearn,[30] T. Muller,[24] R. Mumford,[23] A. Munar,[42] P. Murat,[14] J. Nachtman,[14] S. Nahn,[58] I. Nakamura,[42] I. Nakano,[38] A. Napier,[54] R. Napora,[23] D. Naumov,[35] V. Necula,[15] F. Niell,[32] J. Nielsen,[27] C. Nelson,[14]

 0031-9007/04/93(14)/142001(7)$22.50

T. Nelson,[14] C. Neu,[42] M. S. Neubauer,[7] C. Newman-Holmes,[14] A-S. Nicollerat,[17] T. Nignamov,[43] L. Nodulman,[2] K. Oesterberg,[20] T. Ogawa,[55] S. Oh,[13] Y. D. Oh,[26] T. Ohsugi,[21] T. Okusawa,[39] R. Oldeman,[48] R. Orava,[20] W. Orejudos,[27] C. Pagliarone,[43] F. Palmonari,[43] R. Paoletti,[43] V. Papadimitriou,[51] S. Pashapour,[31] J. Patrick,[14] G. Pauletta,[52] M. Paulini,[10] T. Pauly,[40] C. Paus,[30] D. Pellett,[5] A. Penzo,[52] T. J. Phillips,[13] G. Piacentino,[43] J. Piedra,[9] K. T. Pitts,[22] C. Plager,[6] A. Pompoš,[45] L. Pondrom,[57] G. Pope,[44] O. Poukhov,[12] F. Prakoshyn,[12] T. Pratt,[28] A. Pronko,[15] J. Proudfoot,[2] F. Ptohos,[16] G. Punzi,[43] J. Rademacker,[40] A. Rakitine,[30] S. Rappoccio,[18] F. Ratnikov,[49] H. Ray,[32] A. Reichold,[40] B. Reisert,[14] V. Rekovic,[35] P. Renton,[40] M. Rescigno,[48] F. Rimondi,[3] K. Rinnert,[24] L. Ristori,[43] W. J. Robertson,[13] A. Robson,[40] T. Rodrigo,[9] S. Rolli,[54] L. Rosenson,[30] R. Roser,[14] R. Rossin,[41] C. Rott,[45] J. Russ,[10] A. Ruiz,[9] D. Ryan,[54] H. Saarikko,[20] A. Safonov,[5] R. St. Denis,[18] W. K. Sakumoto,[46] G. Salamanna,[48] D. Saltzberg,[6] C. Sanchez,[37] A. Sansoni,[16] L Santi,[52] S. Sarkar,[48] K. Sato,[53] P. Savard,[31] A. Savoy-Navarro,[14] P. Schemitz,[24] P. Schlabach,[14] E. E. Schmidt,[14] M. P. Schmidt,[58] M. Schmitt,[36] L. Scodellaro,[41] I. Sfiligoi,[16] T. Shears,[28] A. Scribano,[43] F. Scuri,[43] A. Sedov,[45] S. Seidel,[35] Y. Seiya,[39] F. Semeria,[3] L. Sexton-Kennedy,[14] M. D. Shapiro,[27] P. F. Shepard,[44] M. Shimojima,[53] M. Shochet,[11] Y. Shon,[57] I. Shreyber,[34] A. Sidoti,[43] M. Siket,[1] A. Sill,[51] P. Sinervo,[31] A. Sisakyan,[12] A. Skiba,[24] A. J. Slaughter,[14] K. Sliwa,[54] J. R. Smith,[5] F. D. Snider,[14] R. Snihur,[31] S.V. Somalwar,[49] J. Spalding,[14] M. Spezziga,[51] L. Spiegel,[14] F. Spinella,[43] M. Spiropulu,[8] P. Squillacioti,[43] H. Stadie,[24] A. Stefanini,[43] B. Stelzer,[31] O. Stelzer-Chilton,[31] J. Strologas,[35] D. Stuart,[8] A. Sukhanov,[15] K. Sumorok,[30] H. Sun,[54] T. Suzuki,[53] A. Taffard,[22] R. Tafirout,[31] S. F. Takach,[56] H. Takano,[53] R. Takashima,[21] Y. Takeuchi,[53] K. Takikawa,[53] M. Tanaka,[2] R. Takaka,[38] N. Tanimoto,[38] S. Tapprogge,[20] M. Tecchio,[32] P. K. Teng,[1] K. Terashi,[47] R. J. Tesarek,[14] S. Tether,[30] J. Thom,[14] A. S. Thompson,[18] E. Thomson,[37] P. Tipton,[46] V. Tiwari,[10] S. Tkaczyk,[14] D. Toback,[50] K. Tollefson,[33] D. Tonelli,[43] M. Tonnesmann,[33] S. Torre,[43] D. Torretta,[14] W. Trischuk,[31] J. Tseng,[30] R. Tsuchiya,[55] S. Tsuno,[53] D. Tsybychev,[15] N. Turini,[43] M. Turner,[28] F. Ukegawa,[53] T. Unverhau,[18] S. Uozumi,[53] D. Usynin,[42] L. Vacavant,[27] A. Vaiciulis,[46] A. Varganov,[32] E. Vataga,[43] S. Vejcik III,[14] G. Velev,[14] G. Veramendi,[22] T. Vickey,[22] R. Vidal,[14] I. Vila,[9] R. Vilar,[9] I. Volobouev,[27] M. von der Mey,[6] R. G. Wagner,[2] R. L. Wagner,[14] W. Wagner,[24] R. Wallny,[6] T. Walter,[24] T. Yamashita,[38] K. Yamamoto,[39] Z. Wan,[49] M. J. Wang,[1] S. M. Wang,[15] A. Warburton,[31] B. Ward,[18] S. Waschke,[18] D. Waters,[29] T. Watts,[49] M. Weber,[27] W. C. Wester III,[14] B. Whitehouse,[54] A. B. Wicklund,[2] E. Wicklund,[14] H. H. Williams,[42] P. Wilson,[14] B. L. Winer,[37] P. Wittich,[42] S. Wolbers,[14] M. Wolter,[54] M. Worcester,[6] S. Worm,[49] T. Wright,[32] X. Wu,[17] F. Würthwein,[7] A. Wyatt,[29] A. Yagil,[14] U. K. Yang,[11] W. Yao,[27] G. P. Yeh,[14] K. Yi,[23] J. Yoh,[14] P. Yoon,[46] K. Yorita,[55] T. Yoshida,[39] I. Yu,[26] S. Yu,[42] Z. Yu,[58] J. C. Yun,[14] L. Zanello,[48] A. Zanetti,[52] I. Zaw,[19] F. Zetti,[43] J. Zhou,[49] A. Zsenei,[17] and S. Zucchelli[3]

(CDF Collaboration)

[1]*Institute of Physics, Academia Sinica, Taipei, Taiwan 11529, Republic of China*
[2]*Argonne National Laboratory, Argonne, Illinois 60439 USA*
[3]*Istituto Nazionale di Fisica Nucleare, University of Bologna, I-40127 Bologna, Italy*
[4]*Brandeis University, Waltham, Massachusetts 02254 USA*
[5]*University of California at Davis, Davis, California 95616 USA*
[6]*University of California at Los Angeles, Los Angeles, California 90024 USA*
[7]*University of California at San Diego, La Jolla, California 92093 USA*
[8]*University of California at Santa Barbara, Santa Barbara, California 93106 USA*
[9]*Instituto de Fisica de Cantabria, CSIC-University of Cantabria, 39005 Santander, Spain*
[10]*Carnegie Mellon University, Pittsburgh, Pennsylvania 15213 USA*
[11]*Enrico Fermi Institute, University of Chicago, Chicago, Illinois 60637 USA*
[12]*Joint Institute for Nuclear Research, RU-141980 Dubna, Russia*
[13]*Duke University, Durham, North Carolina 27708 USA*
[14]*Fermi National Accelerator Laboratory, Batavia, Illinois 60510 USA*
[15]*University of Florida, Gainesville, Florida 32611 USA*
[16]*Laboratori Nazionali di Frascati, Istituto Nazionale di Fisica Nucleare, I-00044 Frascati, Italy*
[17]*University of Geneva, CH-1211 Geneva 4, Switzerland*
[18]*Glasgow University, Glasgow G12 8QQ, United Kingdom*
[19]*Harvard University, Cambridge, Massachusetts 02138 USA*
[20]*The Helsinki Group: Helsinki Institute of Physics; and Division of High Energy Physics, Department of Physical Sciences, University of Helsinki, FIN-00044, Helsinki, Finland*
[21]*Hiroshima University, Higashi-Hiroshima 724, Japan*
[22]*University of Illinois, Urbana, Illinois 61801 USA*
[23]*The Johns Hopkins University, Baltimore, Maryland 21218 USA*

[24]*Institut für Experimentelle Kernphysik, Universität Karlsruhe, 76128 Karlsruhe, Germany*
[25]*High Energy Accelerator Research Organization (KEK), Tsukuba, Ibaraki 305, Japan*
[26]*Center for High Energy Physics: Kyungpook National University, Taegu 702-701; Seoul National University, Seoul 151-742; and SungKyunKwan University, Suwon 440-746; Korea*
[27]*Ernest Orlando Lawrence Berkeley National Laboratory, Berkeley, California 94720 USA*
[28]*University of Liverpool, Liverpool L69 7ZE, United Kingdom*
[29]*University College London, London WC1E 6BT, United Kingdom*
[30]*Massachusetts Institute of Technology, Cambridge, Massachusetts 02139 USA*
[31]*Institute of Particle Physics, McGill University, Montréal, Quebec H3A 2T8 Canada; and University of Toronto, Toronto, Ontario M5S 1A7 Canada*
[32]*University of Michigan, Ann Arbor, Michigan 48109 USA*
[33]*Michigan State University, East Lansing, Michigan 48824 USA*
[34]*Institution for Theoretical and Experimental Physics, ITEP, Moscow 117259, Russia*
[35]*University of New Mexico, Albuquerque, New Mexico 87131 USA*
[36]*Northwestern University, Evanston, Illinois 60208 USA*
[37]*The Ohio State University, Columbus, Ohio 43210 USA*
[38]*Okayama University, Okayama 700-8530, Japan*
[39]*Osaka City University, Osaka 588, Japan*
[40]*University of Oxford, Oxford OX1 3RH, United Kingdom*
[41]*University of Padova, Istituto Nazionale di Fisica Nucleare, Sezione di Padova-Trento, I-35131 Padova, Italy*
[42]*University of Pennsylvania, Philadelphia, Pennsylvania 19104 USA*
[43]*Istituto Nazionale di Fisica Nucleare, University and Scuola Normale Superiore of Pisa, I-56100 Pisa, Italy*
[44]*University of Pittsburgh, Pittsburgh, Pennsylvania 15260 USA*
[45]*Purdue University, West Lafayette, Indiana 47907 USA*
[46]*University of Rochester, Rochester, New York 14627 USA*
[47]*The Rockefeller University, New York, New York 10021 USA*
[48]*Istituto Nazionale di Fisica Nucleare, Sezione di Roma 1, University di Roma "La Sapienza," I-00185 Roma, Italy*
[49]*Rutgers University, Piscataway, New Jersey 08855 USA*
[50]*Texas A&M University, College Station, Texas 77843 USA*
[51]*Texas Tech University, Lubbock, Texas 79409 USA*
[52]*Istituto Nazionale di Fisica Nucleare, University of Trieste, Udine, Italy*
[53]*University of Tsukuba, Tsukuba, Ibaraki 305, Japan*
[54]*Tufts University, Medford, Massachusetts 02155 USA*
[55]*Waseda University, Tokyo 169, Japan*
[56]*Wayne State University, Detroit, Michigan 48201 USA*
[57]*University of Wisconsin, Madison, Wisconsin 53706 USA*
[58]*Yale University, New Haven, Connecticut 06520 USA*
(Received 26 April 2004; published 27 September 2004)

We report a measurement of the $t\bar{t}$ production cross section using dilepton events with jets and missing transverse energy in $p\bar{p}$ collisions at a center-of-mass energy of 1.96 TeV. Using a 197 ± 12 pb^{-1} data sample recorded by the upgraded Collider Detector at Fermilab, we use two complementary techniques to select candidate events. We compare the number of observed events and selected kinematical distributions with the predictions of the standard model and find good agreement. The combined result of the two techniques yields a $t\bar{t}$ production cross section of $7.0^{+2.4}_{-2.1}(\text{stat})^{+1.6}_{-1.1}(\text{syst}) \pm 0.4(\text{lum})$ pb.

DOI: 10.1103/PhysRevLett.93.142001 PACS numbers: 14.65.Ha, 12.38.Qk, 13.85.Qk

Since the discovery of the top quark [1], experimental attention has turned to the examination of its production and decay properties. Within the standard model (SM), the top quark production cross section is calculated with an uncertainty of $\lesssim 15\%$ [2,3]. Furthermore, in the SM, the top quark decays to a W boson and b quark $\sim 100\%$ of the time. The W subsequently decays to either a pair of quarks or a lepton-neutrino pair. Measuring the rate of the reaction $p\bar{p} \to t\bar{t} \to b\ell^+\nu_\ell \bar{b}\ell'^-\bar{\nu}_{\ell'}$ tests both the production and decay mechanisms of the top quark. A significant deviation from the SM prediction would indicate either a novel production mechanism, e.g., a heavy resonance decaying into $t\bar{t}$ pairs [4], or a novel decay mechanism, e.g., decay into supersymmetric particles [5]. The Collider Detector at Fermilab (CDF) and D0 collaborations previously measured the $t\bar{t}$ production cross section in the dilepton channel during run I of the Fermilab Tevatron [6]. These and related measurements were consistent with SM expectations but suffered large uncertainties due to small event samples.

This Letter describes a measurement of the $t\bar{t}$ cross section in the dilepton channel using data from run II of

the Tevatron taken with the upgraded Collider Detector at Fermilab (CDF II). The data sample corresponds to an integrated luminosity of 197 ± 12 pb^{-1} [7], $\sim 2\times$ that used in run I. Moreover, we expect the higher center-of-mass energy of 1.96 TeV in run II to increase the production of $t\bar{t}$ events by $\sim 30\%$ relative to the run I rate at 1.8 TeV [2,3]. The upgrades to the CDF II detector further increase the $t\bar{t}$ yield with improved lepton acceptance. We perform two complementary analyses of the new data. One, inspired by the technique used by CDF in run I, requires that both leptons be specifically identified as either electrons or muons (DIL analysis). The other technique allows one of the leptons to be identified only as a high-p_T, isolated track (LTRK analysis), thereby significantly increasing the lepton detection efficiency with some increase in expected background events.

The CDF II detector [8] is an azimuthally and forward-backward symmetric apparatus designed to study $p\overline{p}$ reactions at the Tevatron. The detector has a charged particle tracking system immersed in a 1.4 T magnetic field, aligned coaxially with the $p\overline{p}$ beams. A silicon microstrip detector provides tracking over the radial range 1.5 to 28 cm. A 3.1 m long open-cell drift chamber, the central outer tracker, covers the radial range from 40 to 137 cm. The fiducial region of the silicon detector extends to $|\eta| \sim 2$ [9], while the central outer tracker provides coverage for $|\eta| \lesssim 1$.

Segmented electromagnetic and hadronic sampling calorimeters surround the tracking system and measure the energy flow of interacting particles in the pseudorapidity range $|\eta| < 3.6$. This analysis uses the new end plug detectors to identify electron candidates with $1.2 < |\eta| < 2.0$ in addition to the central detectors for lepton candidates with $|\eta| < 1.1$. A set of drift chambers located outside the central hadron calorimeters and another set behind a 60 cm iron shield detect energy deposition from muon candidates with $|\eta| \leq 0.6$. Additional drift chambers and scintillation counters detect muons in the region $0.6 \leq |\eta| \leq 1.0$. Gas Cherenkov counters located in the $3.7 < |\eta| < 4.7$ region [10] measure the average number of inelastic $p\overline{p}$ collisions per bunch crossing and thereby determine the beam luminosity.

The $b\ell^+\nu_\ell \bar{b}\ell'^-\bar{\nu}_{\ell'}$ events under study produce two high-p_T leptons, missing transverse energy ($\not\!\!E_T$) [9] from the undetected neutrinos, and two jets from the hadronization of the b quarks. Additional jets are often produced by initial-state and final-state radiation. A trigger system first identifies candidate events by finding either a central electron or muon candidate with $E_T > 18$ GeV [11], or an end plug electron candidate with $E_T > 20$ GeV [9] in an event with $\not\!\!E_T > 15$ GeV. After full event reconstruction, the candidate event sample is further refined by selection criteria determined *a priori* to minimize the expected statistical and systematic uncertainties of the cross section result.

Both analyses require two oppositely charged leptons with $E_T > 20$ GeV [11]. One lepton, the "tight" lepton, must pass strict lepton identification requirements and be isolated. A lepton is isolated if the total E_T within a cone $\Delta R \equiv \sqrt{(\Delta\eta)^2 + (\Delta\phi)^2} \leq 0.4$, minus the lepton E_T, is $<10\%$ of the lepton E_T [11]. Tight electrons have a well-measured track pointing at an energy deposition in the calorimeter. For electrons with $|\eta| > 1.2$, this track association uses a calorimeter-seeded silicon tracking algorithm [12]. In addition, the candidate's electromagnetic shower profile must be consistent with that expected for electrons. Tight muons must have a well-measured track linked to hits in the muon chambers and energy deposition in the calorimeters consistent with that expected for muons.

The other lepton, the "loose" lepton, is identified differently by the two analyses. The DIL analysis requires the loose lepton to be an electron or muon selected as above, with the exceptions that it need not be isolated and muon identification requirements are relaxed. The LTRK analysis defines a loose lepton as a well-measured, isolated track with $p_T > 20$ GeV/c in the range of $|\eta| < 1$ where the isolation requirement is the tracking analog of the calorimetric isolation employed for tight leptons. These selections add acceptance for dilepton events where electrons or muons pass through gaps in the calorimetry or muon systems. They also contribute acceptance for single prong hadronic decays of the τ lepton from $W \rightarrow \tau\nu$. Consequently, the LTRK analysis derives 20% of its acceptance from taus, compared with 12% for the DIL analysis.

Candidate events must have $\not\!\!E_T > 25$ GeV. To reduce the occurrence of false $\not\!\!E_T$ due to mismeasured jets, we require that the $\not\!\!E_T$ vector point away from any jet. Each analysis takes additional steps to further suppress false $\not\!\!E_T$ arising from mismeasurement of their respective loose leptons. The DIL analysis requires that the $\not\!\!E_T$ vector be at least 20° from the closest lepton. The LTRK analysis corrects the $\not\!\!E_T$ for all loose leptons whenever the associated calorimeter E_T is $<70\%$ of the track p_T. It further rejects events for which the $\not\!\!E_T$ vector lies within 5° of the loose lepton axis. In both analyses, these additional topological cuts are not applied in events with $\not\!\!E_T > 50$ GeV.

The DIL (LTRK) analysis counts jets with $E_T > 15$ (20) GeV detected in $|\eta| < 2.5$ (2.0), where we define a jet as a fixed-cone cluster with a cone size of $R = 0.4$. We correct jet E_T measurements for the effects of calorimeter nonuniformity and absolute energy scale [13].

After removal of cosmic-ray muons and photon-conversion electrons, the dominant backgrounds to dilepton $t\bar{t}$ events are Drell-Yan ($q\bar{q} \rightarrow Z/\gamma^\star \rightarrow \ell^+\ell^-$) production, "fake" leptons in $W \rightarrow \ell\nu$ + jet events where a jet is falsely reconstructed as a lepton candidate, and diboson (WW, WZ, and ZZ) production. Drell-Yan events typically have little $\not\!\!E_T$. Thus, for events with dilepton invari-

ant mass within 15 GeV/c^2 of the Z boson resonance, the DIL analysis imposes a cut on the ratio of $\not\!\!E_T$ to the sum of the jet E_T's projected along the $\not\!\!E_T$ vector, whereas the LTRK analysis tightens its $\not\!\!E_T$ requirement to $\not\!\!E_T >$ 40 GeV. To estimate residual Drell-Yan sample contamination we utilize both a PYTHIA [14] Monte Carlo calculation with detector simulation and the data itself. We select Z boson candidates in the mass range of 76–106 GeV/c^2 and count the number of events passing nominal and Drell-Yan-specific selection criteria. After subtraction of expected non-Drell-Yan contributions, these two numbers provide the normalization for the distribution of expected contributions inside and outside the Z boson mass window. This distribution is obtained as a function of jet multiplicity using a sample of simulated events.

We estimate the fake lepton background contribution by applying a fake lepton rate to a data sample of $W \rightarrow \ell\nu$ + jet events. We determine this fake rate using a large sample of events triggered by at least one jet with $E_T >$ 50 GeV after removing sources of real leptons such as W and Z decays. To check the accuracy and robustness of this estimate we apply our fake lepton rate to different samples with varied physics content: jet data with 20, 70 and 100 GeV trigger thresholds, an inclusive photon sample, and an inclusive electron sample. The observed numbers of fake leptons agree with our fake rate predictions within statistical uncertainties (e.g., 74 observed vs 70 ± 14 predicted for LTRK). An additional check is performed on the like-sign subset of the dilepton sample itself, which is dominantly $W \rightarrow \ell\nu$ + jet events with one fake lepton. We compare the number of observed like-sign events to the like-sign fake background predictions and find good agreement (e.g., five observed vs 6.3 ± 1.4 predicted for DIL).

We determine geometric and kinematic acceptance for the diboson backgrounds using PYTHIA and ALPGEN+HERWIG Monte Carlo calculations [15,16] followed by a simulation of the CDF II detector. We use the CTEQ5L parton distribution functions [17] to model the momentum distribution of the initial-state partons. We normalize the total number of expected events for these processes to their theoretical cross sections: 13.3 pb for WW, 4.0 pb for WZ and 1.5 pb for ZZ [18]. We estimate the uncertainty in these background predictions by comparing different Monte Carlo calculations for the same diboson process. Similarly, we obtain the acceptance for $t\bar{t}$ using a PYTHIA Monte Carlo calculation assuming $m_{top} = 175$ GeV/c^2 and $BR(W \rightarrow \ell\nu) = 10.8\%$.

TABLE II. Summary of systematic uncertainties.

Signal and background uncertainties	LTRK	DIL
Lepton(track) ID	5%(6%)	5%
Jet energy scale—signal	6%	5%
Jet energy scale—background	10%	18–29%
Initial/final state radiation	7%	2%
Parton distribution functions	6%	6%
Monte Carlo generators	5%	6%
WW, WZ, ZZ estimate	20%	20%
Drell-Yan estimate	30%	51%
Fake estimate	12%	41%

We present the predicted and observed numbers of oppositely charged dilepton events versus jet multiplicity in Table I. Good agreement is seen for the background-dominated zero and one-jet events, establishing confidence in the background estimates detailed above. We measure the $t\bar{t}$ production cross section using events with two or more jets. The DIL analysis enhances its signal sensitivity by requiring that H_T, the scalar sum of the lepton p_T, jet E_T, and $\not\!\!E_T$, be >200 GeV.

Systematic uncertainties include uncertainties on the acceptance times efficiency ($a \times \epsilon$) and the background estimates. The dominant uncertainty on $a \times \epsilon$ is due to uncertainties on the jet energy scale and lepton identification/isolation efficiencies. The background uncertainty is dominated by the statistical uncertainty in the Drell-Yan contribution arising from the limited number of Z events with high $\not\!\!E_T$. Table II lists all systematic uncertainties.

Using Table I, the expected signal-to-background ratios are 3.1 for the DIL analysis and 1.7 for the LTRK analysis. The products $a \times \epsilon \times BR(t\bar{t} \rightarrow b\ell^+\nu_\ell \bar{b}\ell'^-\bar{\nu}_{\ell'})$ are

TABLE I. Expected background and $t\bar{t}$ contributions ($m_{\rm top} = 175$ GeV/c^2, $\sigma = 6.7$ pb) compared with observed data.

	LTRK			DIL			
	$N_{\rm jet} = 0$	$N_{\rm jet} = 1$	$N_{\rm jet} \geq 2$	$N_{\rm jet} = 0$	$N_{\rm jet} = 1$	$N_{\rm jet} \geq 2$	$H_T > 200$ GeV
WW, WZ, ZZ	21.8 ± 5.2	6.3 ± 1.5	1.2 ± 0.3	11.4 ± 3.3	3.2 ± 0.9	1.1 ± 0.3	0.7 ± 0.2
Drell-Yan	26.5 ± 9.8	16.4 ± 6.0	4.2 ± 1.6	4.4 ± 1.9	2.9 ± 1.1	1.3 ± 0.5	0.9 ± 0.5
Fakes	16.5 ± 2.4	5.0 ± 1.0	1.5 ± 0.5	3.0 ± 1.2	2.4 ± 1.0	1.5 ± 0.6	1.1 ± 0.5
Total background	64.8 ± 11.3	27.7 ± 6.3	6.9 ± 1.7	18.8 ± 4.0	8.5 ± 1.8	3.9 ± 0.9	2.7 ± 0.7
Expected $t\bar{t}$	0.3 ± 0.2	3.4 ± 0.6	11.5 ± 1.5	0.1 ± 0.0	1.3 ± 0.2	8.5 ± 1.2	8.2 ± 1.1
Total	65.1 ± 11.3	31.1 ± 6.3	18.4 ± 2.3	18.9 ± 4.0	9.8 ± 1.9	12.4 ± 1.6	10.9 ± 1.4
Observed	73	26	19	16	9	14	13

$(0.62 \pm 0.09)\%$ and $(0.88 \pm 0.12)\%$, respectively. The total integrated luminosity is $\int \mathcal{L} dt = 197 \pm 12\ \text{pb}^{-1}$. Hence, the measured cross sections, $(N_{\text{obs}} - N_{\text{bkg}})/[a \times \epsilon \times BR(t\bar{t} \to b\ell^+\nu_\ell \bar{b}\ell'^-\bar{\nu}_{\ell'}) \times \int \mathcal{L}\text{dt}]$, are $8.4^{+3.2+1.5}_{-2.7-1.1} \pm 0.5$ pb for the DIL and $7.0^{+2.7+1.5}_{-2.3-1.3} \pm 0.4$ pb for the LTRK analysis, where the first two uncertainties are statistical and systematic and the third is due to the luminosity determination. We combine these results by dividing the analyses' expected signal and background into three disjoint regions (DIL only, LTRK only, and the overlap). Eleven events are shared between DIL and LTRK. Using the combined $a \times \epsilon \times BR(t\bar{t} \to b\ell^+\nu_\ell \bar{b}\ell'^-\bar{\nu}_{\ell'})$ of 1.03% and accounting for common systematic uncertainties, a joint Poisson likelihood is maximized yielding [19]

$$\sigma_{t\bar{t}} = 7.0^{+2.4}_{-2.1}(\text{stat})^{+1.6}_{-1.1}(\text{syst}) \pm 0.4(\text{lum})\ \text{pb}.$$

We have performed several cross checks. The techniques reproduce the expected W and Z production cross sections (e.g., 252 ± 5 pb measured vs 252 ± 0.9 pb expected for LTRK e + track Z candidates). We compare the number of events with identified bottom quark jets in the signal sample to expectations and find agreement within uncertainties (e.g., seven observed vs 5.9 ± 1.8 expected for DIL). The measured $t\bar{t}$ cross section is stable within its uncertainty to variations of the loose and tight lepton p_T and E_T cuts. When we restrict the analysis to two tight isolated leptons, an expected signal-to-background ratio of 3.4 is achieved with $a \times \epsilon \times BR(t\bar{t} \to b\ell^+\nu_\ell \bar{b}\ell'^-\bar{\nu}_{\ell'}) = (0.34 \pm 0.05)\%$. We observe seven candidates with a predicted background of 1.3 ± 0.5 events, yielding a cross section of $8.5^{+4.5}_{-3.5}(\text{stat})^{+1.8}_{-1.4}(\text{syst}) \pm 0.5(\text{lum})$ pb, in good agreement with the larger samples.

We present key kinematical distributions of the signal sample and find good agreement with the SM, assuming $m_{top} = 175\ \text{GeV}/c^2$. For example, using events from the LTRK analysis, Fig. 1 shows a distribution of the previously defined H_T variable. A Kolmogorov-Smirnov test of this distribution yields a p-value of 75%.

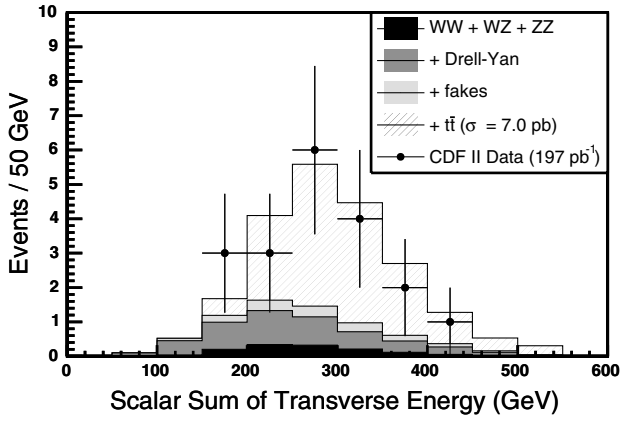

FIG. 1. H_T (defined in text) for events from the LTRK analysis with ≥ 2 jets.

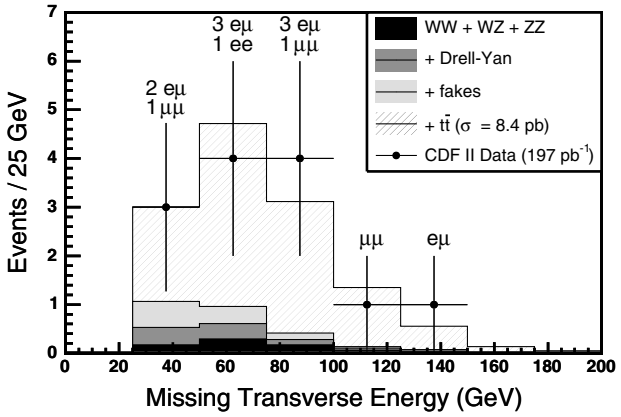

FIG. 2. $\not\!\!E_T$ for events from the DIL analysis with $H_T > 200$ GeV and ≥ 2 jets.

In the DIL analysis, both leptons are always identified as either an electron or a muon. In run I, seven of the nine observed events were eμ, and these events populated the tail of the expected $\not\!\!E_T$ distribution. The expected numbers of ee, $\mu\mu$, and eμ events for the run II DIL analysis, scaled to the 13 total observed events, are 3.3 ± 0.5, 2.8 ± 0.5, and 6.8 ± 0.8, respectively. One ee, three $\mu\mu$, and nine eμ events are observed in the data; the $\not\!\!E_T$ for these events is shown in Fig. 2. A Kolmogorov-Smirnov test of this distribution yields a p-value of 49%.

In summary, we have measured the $t\bar{t}$ production cross section in the dilepton channel to be $7.0^{+2.4}_{-2.1}(\text{stat})^{+1.6}_{-1.1}(\text{syst}) \pm 0.4(\text{lum})$ pb for $m_{\text{top}} = 175\ \text{GeV}/c^2$ [20] using data from the first two years of running of the upgraded Tevatron Collider and CDF II detector. We observe good agreement between the data and the SM prediction in event yield and key kinematic distributions. The measured $t\bar{t}$ cross section agrees well with the full next-to-leading order SM prediction of $6.7^{+0.7}_{-0.9}$ pb [2].

We thank the Fermilab staff and the technical staffs of the participating institutions for their vital contributions. This work was supported by the U.S. Department of Energy and National Science Foundation; the Italian Istituto Nazionale di Fisica Nucleare; the Ministry of Education, Culture, Sports, Science and Technology of Japan; the Natural Sciences and Engineering Research Council of Canada; the National Science Council of the Republic of China; the Swiss National Science Foundation; the A. P. Sloan Foundation; the Bundesministerium fuer Bildung und Forschung, Germany; the Korean Science and Engineering Foundation and the Korean Research Foundation; the Particle Physics and Astronomy Research Council and

the Royal Society, UK; the Russian Foundation for Basic Research; the Comision Interministerial de Ciencia y Tecnologia, Spain; in part by the European Community's Human Potential Programme under contract No. HPRN-CT-20002, Probe for New Physics; by the Research Fund of Istanbul University Project No. 1755/21122001; and by the Research Corporation.

[1] CDF Collaboration, F. Abe *et al.*, Phys. Rev. Lett. **74**, 2626 (1995); D0 Collaboration, S. Abachi *et al.*, Phys. Rev. Lett. **74**, 2632 (1995).
[2] R. Bonciani, S. Catani, M. L. Mangano, and P. Nason, Nucl. Phys. B **529**, 424 (1998); M. Cacciari *et al.*, J. High Energy Phys. 04 (2004) 068.
[3] N. Kidonakis and R. Vogt, Phys. Rev. D **68**, 114014 (2003).
[4] C. T. Hill and S. J. Parke, Phys. Rev. D **49**, 4454 (1994).
[5] H. P. Nilles, Phys. Rep. **110**, 1 (1984); H. E. Haber and G. L. Kane, Phys. Rep. **117**, 75 (1985).
[6] D0 Collaboration, B. Abbott *et al.*, Phys. Rev. Lett. **79**, 1203 (1997); CDF Collaboration, F. Abe *et al.*, Phys. Rev. Lett. **80**, 2779 (1998).
[7] S. Klimenko *et al.*, Fermilab Report No. FERMILAB-FN-0741 2003 (unpublished); D. Acosta *et al.*, Nucl. Instrum. Methods Phys. Res., Sect. A **494**, 57 (2002).
[8] CDF II Collaboration, Fermilab Report No. FERMILAB-PUB-96/390-E 1996 (unpublished).
[9] We use a cylindrical coordinate system about the beam axis in which θ is the polar angle, ϕ is the azimuthal angle, and $\eta \equiv -\ln\tan(\theta/2)$. $E_T \equiv E\sin\theta$ and $p_T \equiv p\sin\theta$ where E is energy measured by the calorimeter and p is momentum measured by the spectrometer. $\not\!\!E_T \equiv -\sum_i \mathrm{E_T^i}\nu_i$, where n_i is the unit vector in the azimuthal plane that points from the beam line to the ith calorimeter tower.
[10] D. Acosta *et al.*, Nucl. Instrum. Methods Phys. Res., Sect. A **461**, 540 (2001).
[11] For muons, transverse momentum (not energy) is used.
[12] C. Issever, AIP Conf. Proc. **670**, 371 (2003).
[13] The absolute energy correction ranges from ~1.3 at low energies to ~1.1 at high energies.
[14] T. Sjöstrand *et al.*, Comput. Phys. Commun. **135**, 238 (2001).
[15] M. L. Mangano *et al.*, J. High Energy Phys. 07 (2003) 001.
[16] G. Marchesini *et al.*, Comput. Phys. Commun. **67**, 465 (1992); G. Corcella *et al.*, J. High Energy Phys. 01 (2001) 010.
[17] H. L. Lai *et al.*, Eur. Phys. J. C **12**, 375 (2000).
[18] J. M. Campbell and R. K. Ellis, Phys. Rev. D **60**, 113006 (1999).
[19] The individual cross sections (DIL only, LTRK only, and overlap) range from ~4–10 pb which aggregately yield the combined result of 7.0 pb.
[20] The dependence of the measured cross section on m_{top} is $-(+)0.04$ pb per GeV/c^2 greater (less) than the assumed value of 175 GeV/c^2.